Hindawi
Mathematical Problems in Engineering
Volume 2019, Article ID 1504308, 9 pages
https://doi.org/10.1155/2019/1504308

Research Article

Multitarget Parameter Estimation of Monopulse Radar Based on RJ-MCMC Algorithm

Jian Gong,[1,2,3] **Yiduo Guo**,[2] **Hui Yuan**,[2] **and Qun Wan**[1]

[1] *University of Electronic Science and Technology of China, Chengdu, Sichuan, 611731, China*
[2] *Air Force Engineering University, Xi'an, Shaanxi, 710051, China*
[3] *TongFang Electronic Science and Technology Co. Ltd., Jiujiang Jiangxi, 332007, China*

Correspondence should be addressed to Jian Gong; wcyls@163.com

Received 29 June 2018; Revised 13 November 2018; Accepted 21 November 2018; Published 6 January 2019

Academic Editor: Nazrul Islam

A multiple parameter estimation method based on RJ-MCMC for multiple nondiscernible targets is proposed in this paper. Different from the traditional estimation methods, the proposed method can simultaneously complete the joint estimation of the target number and the target location parameters. More importantly, the method proposed in this chapter is applicable to many situations with different power and nondistinguishable target. The simulation results show that the method proposed in this chapter requires less observation time to obtain similar and even better estimation performance than the ML-MDL method, which is of great significance for real-time processing.

1. Introduction

In the process of fighter penetration, as shown in Figure 1, a two-tier echelon and a team's wedge formation are usually used [1].

It can be seen that two or more than two targets are likely to exist in the same distance-angle resolution unit of the radar when the target is launched with a double "Echelon" or a team 's "wedge" formation. With the influence of side lobe jamming and false target jamming [2–5], radar's display on the two-dimensional display of distance angle is shown in Figure 2. The red pentagram represents the target that radar is detecting or tracking, and the dot represents other targets or false targets.

From Figure 2, we can see that, during the penetration process, many false targets may be observed in the range angle dimension of radar. The black dots represent the false targets in the sidelobe region, which can be suppressed by the side lobe countermeasures. The blue dots represent the false targets in the different range resolution units in the radar main beam resolution unit and can be identified or suppressed by the method of distance dimension false target interference. However, the false targets (green dots) in the same distance and angle resolution units are still possible to cause interference to the radar angle measurement and tracking system. Serious deviation will occur when the angle of the target is estimated by using the traditional single pulse processing.

From the spatial domain, the composite jamming described above can deceive monopulse radar from a multisource coherent/incoherent angle. The solution to this problem from the beam is the angle superresolution method based on the improved monopulse processing method, and it mainly includes complex monopulse processing method [6–10], parameter estimation method based on joint bin processing (JBP) [11, 12], and maximum likelihood (ML) estimation. The complex monopulse processing method assumes that the target just falls on the sampling point of matched filter and only uses one matched filter to sample information, so it can only solve the problem of angle estimation of up to two indistinguishable targets. The ML estimation algorithm based on JBP model is computationally intensive and easy to fall into local extremum. When the number of samples is small and the SNR is low, the minimum description length (MDL) criterion is used to estimate the number of targets in the beam and it is very easy to fail. The standard MCMC method

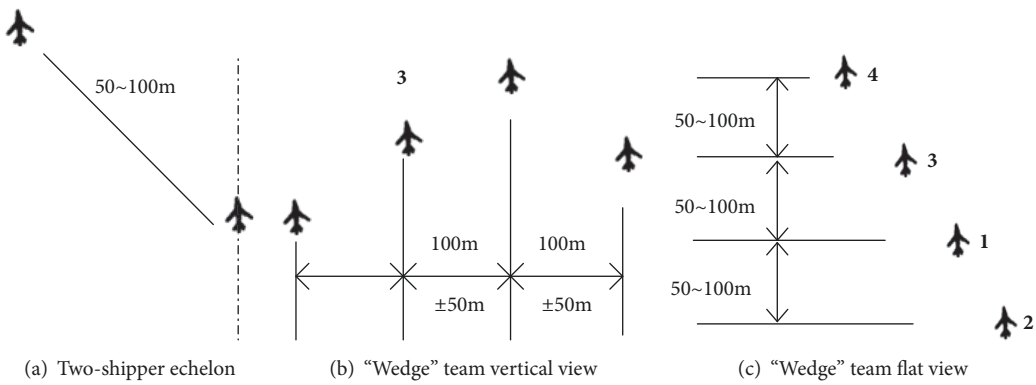

Figure 1: The fighting order of fighter plane.

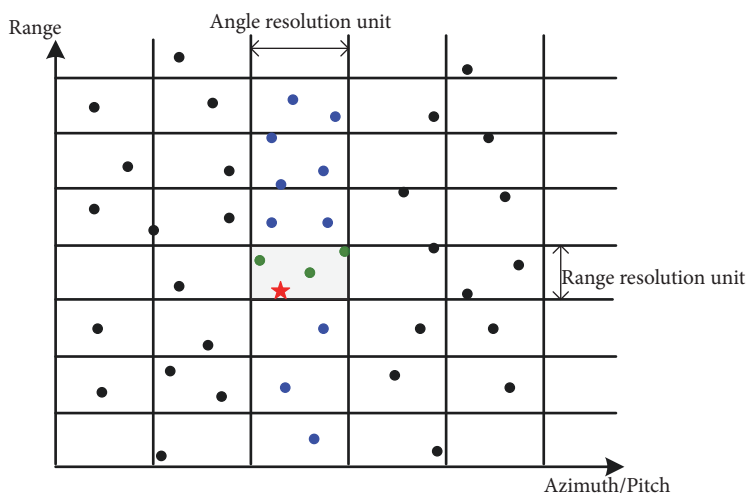

Figure 2: Radar range-angle two-dimensional display diagram.

cannot "jump" between subspaces of different dimensions, so it does not have the ability to estimate the number of targets. A direct solution is similar to the method proposed by [11, 12]. In order to get the target parameters estimation, the order MCMC sampling algorithm is run independently and the number of targets is fixed at each time. Then the number of targets is judged by MDL criterion. However, there is no substantial improvement in the amount of computation and estimation accuracy. Therefore, in this paper, we use RJ-MCMC method to jointly estimate target number and target position parameters. RJ-MCMC method can "jump" from different dimension space when the dimension of parameter space changes; that is, it can directly sample according to the joint distribution of A and finally get the estimation results of target number and target position parameters.

The remainder of this paper is organized as follows. In Section 2, the joint bin processing (JBP) model is established. Then, the prior and posterior distributions of Bayesian parameter estimation are derived in Section 3, followed by a multitarget parameter estimation algorithm for monopulse radar Based on RJ-MCMC is proposed in Section 4. Some simulations are conducted to verify the performance of the proposed method in Section 5. Finally, we conclude the paper in Section 6.

2. Joint Bin Processing Model

Before giving the model, we first make the following assumptions:

(I) Assuming that the target model is a point target model, the extended target is not considered.

(II) When the noise is not considered, the output of matched filter is triangular waveform; that is, the radar transmits the signal with rectangular envelope.

(III) The sampling interval after matched filtering is pulse width T, which means that a target can only appear in its adjacent matched filtering sampling points.

Figure 3 shows the "leakage" model of two targets at two adjacent sampling points. ΔT represents the time offset of the real target position relative to the sampling point 1. $x = a\cos(\phi)$ (or $x = a\sin(\phi)$) is the peak amplitude of the target echo in the same phase (or quadrature) channel after matched filtering. If $\alpha = \Delta T/T$ is defined, the amplitude of the target

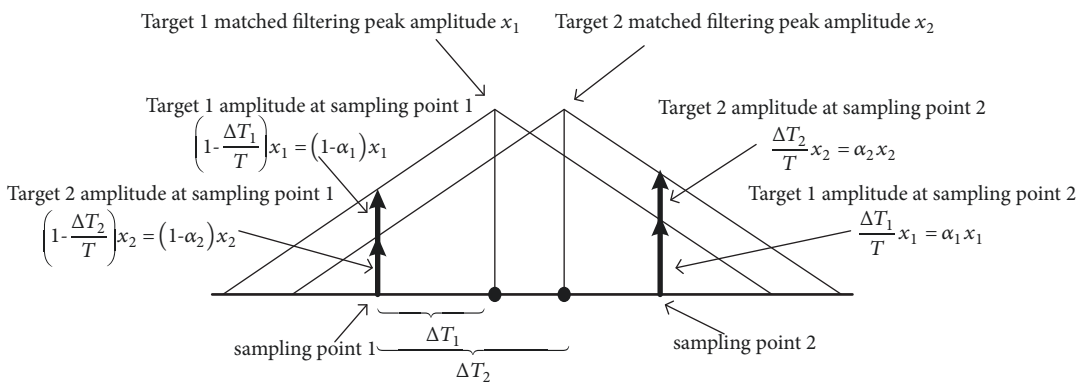

Figure 3: Two targets at two adjacent sampling points "leakage" model.

echo at the first and second sampling points is $(1-\alpha)x$ and αx, respectively.

Suppose that there are k targets between the two sampling points. When the radar launches the first pulse, we can get the target's observed values at two sampling points, as shown in Formula (1):

$$\begin{aligned}
s_{i1}(m) &= \sum_{j}^{k}\left(1-\alpha_j\right)x_j(m)+n_{si1}(m)\\
s_{i2}(m) &= \sum_{j}^{k}\alpha_j x_j(m)+n_{si2}(m)\\
d_{ai1}(m) &= \sum_{j}^{k}\left(1-\alpha_j\right)\eta_{aj}x_j(m)+n_{dai1}(m)\\
d_{ai2}(m) &= \sum_{j}^{k}\alpha_j\eta_{aj}x_j(m)+n_{ai2}(m)\\
d_{ei1}(m) &= \sum_{j}^{k}\left(1-\alpha_j\right)\eta_{ej}x_j(m)+n_{ei1}(m)\\
d_{ei2}(m) &= \sum_{j}^{k}\alpha_j\eta_{ej}x_j(m)+n_{ei2}(m)
\end{aligned} \tag{1}$$

where, $\{\alpha_j\}_{j=1}^{k}$, $\{\eta_{aj}\}_{j=1}^{k}$, and $\{\eta_{ej}\}_{j=1}^{k}$ are the parameters to be estimated, respectively, the k target in the subgate in relative distance, azimuth, and elevation information. $\{s_{i1}(m)\}_{m=1}^{M}$, $\{d_{ai1}(m)\}_{m=1}^{M}$, and $\{d_{ei1}(m)\}_{m=1}^{M}$ are the observation data for sum, azimuth, and elevation difference channels for sampling point 1. $\{s_{i2}(m)\}_{m=1}^{M}$, $\{d_{ai2}(m)\}_{m=1}^{M}$, and $\{d_{ei2}(m)\}_{m=1}^{M}$ are the observation data for sum, azimuth, and elevation difference channels for sampling point 2. $x_j(m)$ is the matching pulse output of the m pulse of the j target. $\{x_j(m)\}_{m=1}^{M}$ obeys the Gauss distribution of zero mean and σ_{tj}^2 variance.

The observation model given by Formula (1) is expressed as vector matrix form:

$$\begin{aligned}
&\boldsymbol{Z}(:,m)\\
&=\left[s_i(m)\ \ s_q(m)\ \ d_{ai}(m)\ \ d_{aq}(m)\ \ d_{ei}(m)\ \ d_{eq}(m)\right]^{\mathrm{T}}\\
&=\boldsymbol{D}\boldsymbol{X}(:,m)+\boldsymbol{W}(:,m)
\end{aligned} \tag{2}$$

where

$$\boldsymbol{D}=\begin{bmatrix}
1-\alpha_1 & 1-\alpha_2 & \cdots & 1-\alpha_k\\
\alpha_1 & \alpha_2 & \cdots & \alpha_k\\
(1-\alpha_1)\eta_{a1} & (1-\alpha_2)\eta_{a2} & \cdots & (1-\alpha_k)\eta_{ak}\\
\alpha_1\eta_{a1} & \alpha_2\eta_{a2} & \cdots & \alpha_k\eta_{ak}\\
(1-\alpha_1)\eta_{e1} & (1-\alpha_2)\eta_{e2} & \cdots & (1-\alpha_k)\eta_{ek}\\
\alpha_1\eta_{e1} & \alpha_2\eta_{e2} & \cdots & \alpha_k\eta_{ek}
\end{bmatrix},$$
$$\boldsymbol{W}=\begin{bmatrix}
n_{si1}(1) & n_{si1}(2) & \cdots & n_{si1}(M)\\
n_{si2}(1) & n_{si2}(2) & \cdots & n_{si2}(M)\\
n_{dai1}(1) & n_{dai1}(2) & \cdots & n_{dai1}(M)\\
n_{dai2}(1) & n_{dai2}(2) & \cdots & n_{dai2}(M)\\
n_{dei1}(1) & n_{dei1}(2) & \cdots & n_{dei1}(M)\\
n_{dei2}(1) & n_{dei2}(2) & \cdots & n_{dei2}(M)
\end{bmatrix}. \tag{3}$$

Combined with the M group observations, we can get the following:

$$\boldsymbol{z}=\boldsymbol{Z}(:)=\boldsymbol{R}\left(\boldsymbol{s}_k\right)\boldsymbol{a}_k+\boldsymbol{v} \tag{4}$$

where $\boldsymbol{s}_k \triangleq [\boldsymbol{\alpha}^{\mathrm{T}};\boldsymbol{\eta}_a^{\mathrm{T}};\boldsymbol{\eta}_e^{\mathrm{T}}]$ is a set of unknown parameters, $\boldsymbol{\alpha}=[\alpha_1\ \alpha_2\ \cdots\ \alpha_k]^{\mathrm{T}}$, $\boldsymbol{\eta}_a=[\eta_{a1}\ \eta_{a2}\ \cdots\ \eta_{ak}]^{\mathrm{T}}$, $\boldsymbol{\eta}_e=[\eta_{e1}\ \eta_{e2}\ \cdots\ \eta_{ek}]^{\mathrm{T}}$, and $(\cdot)^{\mathrm{T}}$ indicates a transposing of a matrix or vector. $\boldsymbol{z}=\boldsymbol{Z}(:)$, $\boldsymbol{a}_k=\boldsymbol{X}(:)$, and $\boldsymbol{v}=\boldsymbol{W}(:)$, respectively, represent the vectors of observation matrix $\boldsymbol{Z}$, amplitude matrix $\boldsymbol{X}$, and noise matrix $\boldsymbol{W}$.

3. Bayesian Parameter Estimation Method

3.1. Prior Distribution Hypothesis. Because the actual location of the target is unknown, it can be assumed that it is evenly distributed between two consecutive sampling points [13]:

$$\begin{aligned} \alpha_j &\sim U(0,1), \\ \eta_{aj} &\sim U(-1,1), \\ \eta_{ej} &\sim U(-1,1) \\ & j = 1, 2, \cdots k \end{aligned} \tag{5}$$

Because the independence between targets, the parameter space of $\boldsymbol{s}_k$ can be expressed as

$$\Phi_k \triangleq (0,1)^k \times (-1,1)^k \times (-1,1)^k \tag{6}$$

Under the condition that the number of targets is k, the location parameters of all k targets are

$$p(\boldsymbol{s}_k \mid k) = \prod_{j=1}^{k} \left(\frac{1}{1-0} \cdot \frac{1}{1-(-1)} \cdot \frac{1}{1-(-1)} \right) = \frac{1}{4^k} \tag{7}$$

The prior distribution of target number k obeys censored Poisson distribution:

$$p(k) \propto \frac{\Lambda^k}{k!} e^{-\Lambda}, \quad k \in [0, k_{\max}] \tag{8}$$

Document [14] points out that the number of targets that can be distinguished within the beam cannot exceed 5 at most, that is, $k_{\max} = 5$. Λ can be understood as the number of desired targets, and its influence can be eliminated by calculating Bias factor $p(\boldsymbol{z} \mid k_1)/p(\boldsymbol{z} \mid k_2)$.

Under the condition of $(k, \boldsymbol{s}_k)$ is known, the target amplitude $\boldsymbol{a}_k$ obeys the Gauss distribution whose mean value is zero and the covariance is $\sigma_k^2 \boldsymbol{\Sigma}$. $\boldsymbol{\Sigma} = \operatorname{diag}(\underbrace{\boldsymbol{\Sigma}_k, \cdots, \boldsymbol{\Sigma}_k}_{M\uparrow})$, $\boldsymbol{\Sigma}_k^{-1} = \delta^{-2} \boldsymbol{I}_{k\times k}$. δ^2 denotes the expected signal-to-noise ratio and obeys the conjugate Gama prior distribution, that is,

$$\delta^2 \sim Ig\left(\frac{\alpha_0}{2}, \frac{\beta_0}{2} \right) \tag{9}$$

The noise power σ_k^2 can also be assumed to obey the conjugate Gama prior distribution:

$$\sigma_k^2 \sim Ig\left(\frac{\upsilon_0}{2}, \frac{\gamma_0}{2} \right) \tag{10}$$

And α_0, β_0, υ_0, and γ_0 stand for superparameters.

3.2. Posteriori Distribution Derivation. According to Bayes principle, the joint posterior distribution of all parameters is

$$p(k, \boldsymbol{\theta}_k \mid \boldsymbol{z}) = \frac{p(k, \boldsymbol{\theta}_k, \boldsymbol{z})}{p(\boldsymbol{z})} \propto p(\boldsymbol{z} \mid k, \boldsymbol{\theta}_k)\, p(k, \boldsymbol{\theta}_k) \tag{11}$$

where $p(\boldsymbol{z} \mid k, \boldsymbol{\theta}_k)$ is a likelihood function, which can be obtained by Formula (4), that is,

$$p(\boldsymbol{z} \mid k, \boldsymbol{\theta}_k) = \left(2\pi\sigma_k^2\right)^{-6M/2} \exp\left[-\frac{\left\| \boldsymbol{z} - \boldsymbol{R}(\boldsymbol{s}_k)\, \boldsymbol{a}_k \right\|^2}{2\sigma_k^2} \right] \tag{12}$$

The joint posterior distribution of $(k, \boldsymbol{\theta}_k)$ can be obtained by chain decomposition method, that is,

$$p(k, \boldsymbol{\theta}_k) = p\left(k, \boldsymbol{s}_k, \boldsymbol{a}_k, \sigma_k^2\right) = p\left(k, \boldsymbol{s}_k, \boldsymbol{a}_k \mid \sigma_k^2\right) p\left(\sigma_k^2\right) \tag{13}$$

According to the prior distribution hypothesis, we can get the joint distribution of $(k, \mathbf{s}_k, \mathbf{a}_k)$ as follows:

$$\begin{aligned} p\left(k, \boldsymbol{s}_k, \boldsymbol{a}_k \mid \sigma_k^2\right) \propto{}& \frac{\Lambda^k e^{-\Lambda}}{k!} \cdot \frac{1}{4^k} \\ & \cdot \frac{\exp\left(-\boldsymbol{a}_k^T \Sigma^{-1} \boldsymbol{a}_k / 2\sigma_k^2\right)}{\left|2\pi\sigma_k^2 \Sigma\right|^{1/2}} \end{aligned} \tag{14}$$

Using the above assumptions and derivation, we can get the following:

$$\begin{aligned} p(k, \boldsymbol{\theta}_k \mid \boldsymbol{z}) &\propto p(\boldsymbol{z} \mid k, \boldsymbol{\theta}_k)\, p\left(k, \boldsymbol{s}_k, \boldsymbol{a}_k \mid \sigma_k^2\right) p\left(\sigma_k^2\right) \\ &\propto \left(2\pi\sigma_k^2\right)^{-6M/2} \exp\left[-\frac{\left(\gamma_0 + \boldsymbol{z}^T \boldsymbol{P}_k \boldsymbol{z}\right)}{2\sigma_k^2} \right] \left(\sigma_k^2\right)^{-\upsilon_0/2-1} \\ &\quad \cdot \frac{\Lambda^k}{k!} \cdot \frac{1}{4^k} \cdot \left|2\pi\sigma_k^2 \Sigma\right|^{-1/2} \\ &\quad \cdot \exp\left[-\frac{\left(\boldsymbol{a}_k - \boldsymbol{n}_k\right)^T \boldsymbol{N}_k^{-1} \left(\boldsymbol{a}_k - \boldsymbol{n}_k\right)}{2\sigma_k^2} \right] \end{aligned} \tag{15}$$

where $\boldsymbol{N}_k^{-1} = \boldsymbol{\Sigma}^{-1} + \boldsymbol{R}^T(\boldsymbol{s}_k)\boldsymbol{R}(\boldsymbol{s}_k)$, $\boldsymbol{n}_k = \boldsymbol{N}_k \boldsymbol{R}^T(\boldsymbol{s}_k)\boldsymbol{z}$, and $\boldsymbol{P}_k = \boldsymbol{I} - \boldsymbol{R}(\boldsymbol{s}_k)\boldsymbol{N}_k \boldsymbol{R}^T(\boldsymbol{s}_k)$.

According to the prior distribution hypothesis of $\boldsymbol{a}_k$ and σ_k^2, we can eliminate the $\boldsymbol{a}_k$ and σ_k^2 in Formula (15) and finally get the joint posterior distribution of $(k, \boldsymbol{s}_k)$ as

$$\begin{aligned} & p(k, \mathbf{s}_k \mid \mathbf{z}) \\ & \quad \propto \left(\frac{\gamma_0 + \mathbf{z}^T \mathbf{P}_k \mathbf{z}}{2} \right)^{-(6M+\upsilon_0)/2} \frac{\left[\Lambda / \left(1 + \delta^2\right)^{M/2} \right]^k}{k! \cdot 4^k} \end{aligned} \tag{16}$$

Because the location parameters of each target are independent of each other, if k, $\boldsymbol{s}_{ki}$, and $\boldsymbol{z}$ are known, then the location parameter vector $\boldsymbol{s}_k(:, i)$ of the i target follows the following distribution:

$$p\left(\boldsymbol{s}_k(:, i) \mid k, \boldsymbol{s}_{ki}, \boldsymbol{z}\right) \propto \left(\frac{\gamma_0 + \boldsymbol{z}^T \boldsymbol{P}_k \boldsymbol{z}}{2} \right)^{-(6M+\upsilon_0)/2} \tag{17}$$

where $\boldsymbol{s}_{ki} \triangleq \boldsymbol{s}_k \setminus \boldsymbol{s}_k(:, i)$ represents all the parameters except column i in matrix $\boldsymbol{s}_k$, $1 \le i \le k$.

4. Parameter Estimation Algorithm Based on RJ-MCMC

RJ-MCMC is essentially a generalized state space MH algorithm [15, 16]. It includes three states: the birth process, the destruction process, and the renewal process. The corresponding probabilities are b_k, d_k, and u_k respectively, and for all $k \in [0, k_{\max}]$, there are $b_k + d_k + u_k = 1$. b_k and d_{k+1} are as follows:

$$b_k \triangleq c \cdot \min\left\{1, \frac{p(k+1)}{p(k)}\right\}$$
$$d_{k+1} \triangleq c \cdot \min\left\{1, \frac{p(k)}{p(k+1)}\right\} \tag{18}$$

where $c = 0.5$ is a jump parameter, which controls the jump probability of the renewal process to the birth and death process.

The main process of the RJ-MCMC algorithm can be described as follows [17].

Step 1. Initialization: $(k^{(0)}, \boldsymbol{\theta}_k^{(0)}) \in \Theta$

Step 2. The ith iteration process is as follows:

Sample $u \sim U(0,1)$;

If $u \le b_{k^{(i)}}$, execute the birth process;

Otherwise, if $u \le (b_{k^{(i)}} + d_{k^{(i)}})$, then execute the destruction process;

Otherwise, execute the renewal process.

Step 3. $i \longleftarrow i+1$, and return to Step 2.

4.1. The Birth Process. Suppose the current parameter space is $(k, \boldsymbol{s}_k)$ and $k < k_{\max}$. After randomly generating a new target, the parameter space becomes $(k+1, \boldsymbol{s}_{k+1})$. According to the prior distribution of target parameters, we can get the recommended distribution of birth process and extinction process, that is,

$$q(k+1, \boldsymbol{s}_{k+1} \mid k, \boldsymbol{s}_k) = b_k \cdot \frac{1}{1-0} \cdot \frac{1}{1-(-1)} \cdot \frac{1}{1-(-1)} = \frac{b_k}{4} \tag{19}$$

$$q(k, \boldsymbol{s}_k \mid k+1, \boldsymbol{s}_{k+1}) = \frac{d_{k+1}}{k+1} \tag{20}$$

Combining formulas (19) and (20), we can get the reception rate and the reception probability are

$$\begin{aligned} r_{\text{birth}} &= \frac{p(k+1, \boldsymbol{s}_{k+1} \mid \boldsymbol{z})}{p(k, \boldsymbol{s}_k \mid \boldsymbol{z})} \cdot \frac{q(k, \boldsymbol{s}_k \mid k+1, \boldsymbol{s}_{k+1})}{q(k+1, \boldsymbol{s}_{k+1} \mid k, \boldsymbol{s}_k)} \\ &= \left(\frac{\gamma_0 + \boldsymbol{z}^T \boldsymbol{P}_k \boldsymbol{z}}{\gamma_0 + \boldsymbol{z}^T \boldsymbol{P}_{k+1} \boldsymbol{z}}\right)^{(6M+\nu_0)/2} \cdot \frac{1}{(1+\delta^2)^{M/2}} \\ &\quad \cdot \frac{1}{k+1} \\ A_{\text{birth}} &= \min\{1, r_{\text{birth}}\} \end{aligned} \tag{21}$$

The specific steps of the birth process can described as below.

Step 1. A new target is generated randomly according to the prior distribution of target location parameters.

Step 2.

Calculate the A_{birth} by the Formula (21);

Take sample $u \sim U(0,1)$.

Step 3.

If $u \le A_{\text{birth}}$, the state of Markov chain is changed to $\{k+1, \boldsymbol{s}_{k+1}\}$;

Otherwise, the original state $\{k, \boldsymbol{s}_k\}$ is kept.

4.2. The Destruction Process. Suppose the current parameter space is $\{k+1, \boldsymbol{s}_{k+1}\}$, $k > 0$. Then we remove one target randomly and get the new parameter space $\{k, \boldsymbol{s}_k\}$. Similar to the birth process, we can get the reception rate and the reception probabilities of the destruction process are

$$\begin{aligned} r_{\text{death}} &= \frac{p(k-1, \boldsymbol{s}_{k-1} \mid \boldsymbol{z})}{p(k, \boldsymbol{s}_k \mid \boldsymbol{z})} \cdot \frac{q(k, \boldsymbol{s}_k \mid k-1, \boldsymbol{s}_{k-1})}{q(k-1, \boldsymbol{s}_{k-1} \mid k, \boldsymbol{s}_k)} \\ &= \left(\frac{\gamma_0 + \boldsymbol{z}^T \boldsymbol{P}_k \boldsymbol{z}}{\gamma_0 + \boldsymbol{z}^T \boldsymbol{P}_{k-1} \boldsymbol{z}}\right)^{(6M+\nu_0)/2} \cdot \left(1+\delta^2\right)^{M/2} \cdot k \\ A_{\text{death}} &= \min\{1, r_{\text{death}}\} \end{aligned} \tag{22}$$

The specific steps of the destruction process can described as below.

Step 1. Remove one target randomly from the existing $k+1$ goals.

Step 2.

Calculate the A_{death} by Formula (22);

Take sample $u \sim U(0,1)$.

Step 3.

If $u \le A_{\text{death}}$, the state of Markov chain is changed to $\{k, \boldsymbol{s}_k\}$;

Otherwise, the original state $\{k+1, \boldsymbol{s}_{k+1}\}$ is kept.

Table 1: The mixed MH algorithm.

For $j = 1, \cdots, k$

Take sample $u_1 \sim U(0,1)$;

If $u_1 < \lambda$ $(0 < \lambda < 1)$, take the proposal distribution $q_1(\boldsymbol{s}_k^*(:,j) \mid \boldsymbol{s}_k(:,j))$. And the target distribution of $p(\boldsymbol{s}_k(:,j) \mid \boldsymbol{z}, \boldsymbol{s}_{kj})$ as invariant distribution of $\pi(\boldsymbol{s}_k(:,j))$, MH performed a step sampling;

Else, take the proposal distribution $q_2(\boldsymbol{s}_k^*(:,j) \mid \boldsymbol{s}_k(:,j))$, And the target distribution of $p(\boldsymbol{s}_k(:,j) \mid \boldsymbol{z}, \boldsymbol{s}_{kj})$ as invariant distribution of $\pi(\boldsymbol{s}_k(:,j))$, MH performed a step sampling;

End if

End for

Table 2: Two consecutive sampling points between the 5 goals of the position.

Target number	Sub gate distance	Azimuth	Pitch
1	0.15	-0.8	-0.9
2	0.35	-0.6	0.7
3	0.55	0.1	-0.4
4	0.75	0.5	0.8
5	0.95	0.9	-0.8

4.3. The Renewal Process. The renewal process is actually a standard MCMC sampling process. In this article, we use mixed MH sampling to generate $\boldsymbol{s}_k$, in order to achieve optimal search and traversal of target location parameter space, as shown in Table 1.

The receiving probability of the update process can be obtained as

$$A_{\text{update}} = \min\left\{1, r_{\text{update}}\right\} = \min\left\{1, \left(\frac{\gamma_0 + \boldsymbol{z}^T \boldsymbol{P}_k \boldsymbol{z}}{\gamma_0 + \boldsymbol{z}^T \boldsymbol{P}_k^* \boldsymbol{z}}\right)^{(6M+\nu_0)/2} \frac{q_i\left(\boldsymbol{s}_{k,j} \mid \boldsymbol{s}_{k,j}^*\right)}{q_i\left(\boldsymbol{s}_{k,j}^* \mid \boldsymbol{s}_{k,j}\right)}\right\} \quad (23)$$

To determine the convergence of the direct determination method, calculate a mean ergodic every 50 iterations, if the absolute value of three consecutive mean calculation results the difference of the control coefficient error is less than the set, to determine the estimate convergence and to stop the iteration.

5. Computer Simulation Results

Assume there is a maximum of 5 goals between two consecutive sampling assumptions. Location parameters and their settings in the document [11] are the same, as shown in Table 2. Given the hyperparameters and other related parameters as [12], $\alpha_0 = 2, \beta_0 = 10, \nu_0 = \gamma_0 = 0.1, \lambda = 0.2$, and $\boldsymbol{\Sigma}_{q_2} = \boldsymbol{I}/(30M)$. Monte Carlo simulation 200 times is to get the following results. We will call the method in the document [11, 14] abbreviated as ML-MDL.

Experiment 1 (performance analysis for estimating target location parameters). When the target has the same power, Figures 4–6 show the wavelet door relative distance of target 1, azimuth, and pitch angle estimation accuracy, under different SNR conditions and different real target number conditions.

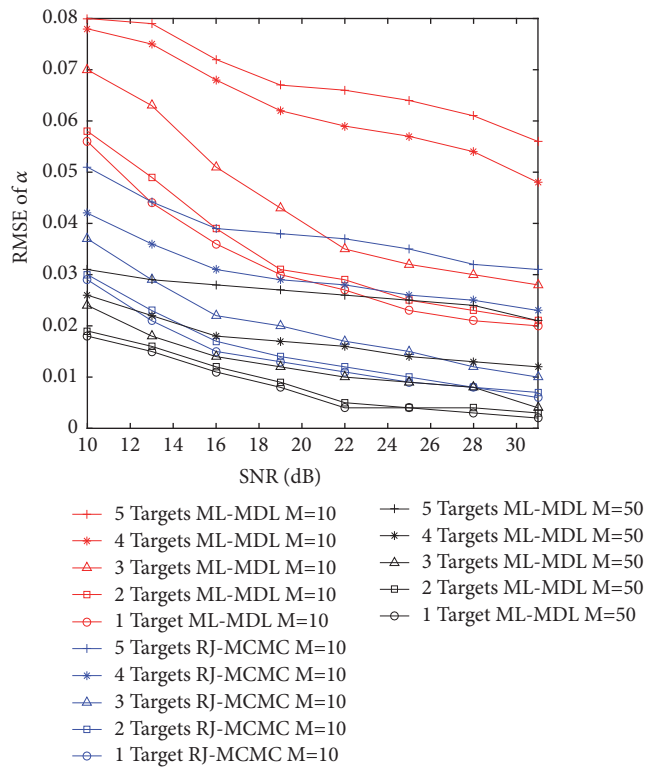

Figure 4: RMSE of α estimation under the same power, different target numbers, and different SNR conditions.

From Figures 4–6, we can see that, in any case, the estimated RMSE will increase as the number of real targets increases. For ML-MDL method, increasing the number of observation pulses can improve the accuracy of parameter estimation to a certain extent. In addition, we can see that the estimation performance of the RJ-MCMC method is between the other two cases under the condition of 10 subpulses. That is to say, compared with the ML-MDL method, the RJ-MCMC method has better estimation performance under the same sub pulse number condition.

Experiment 2 (RMSE estimation of two targets under different SNR conditions). Suppose there are two different power targets and the SNR of target 1 changes from 15dB to 30dB

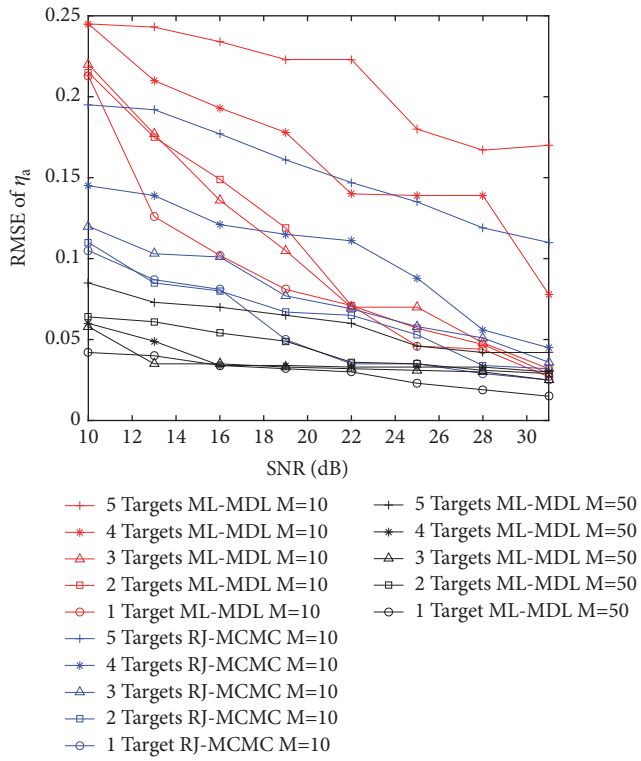

Figure 5: RMSE of η_a estimation under the same power, different target numbers, and different SNR conditions.

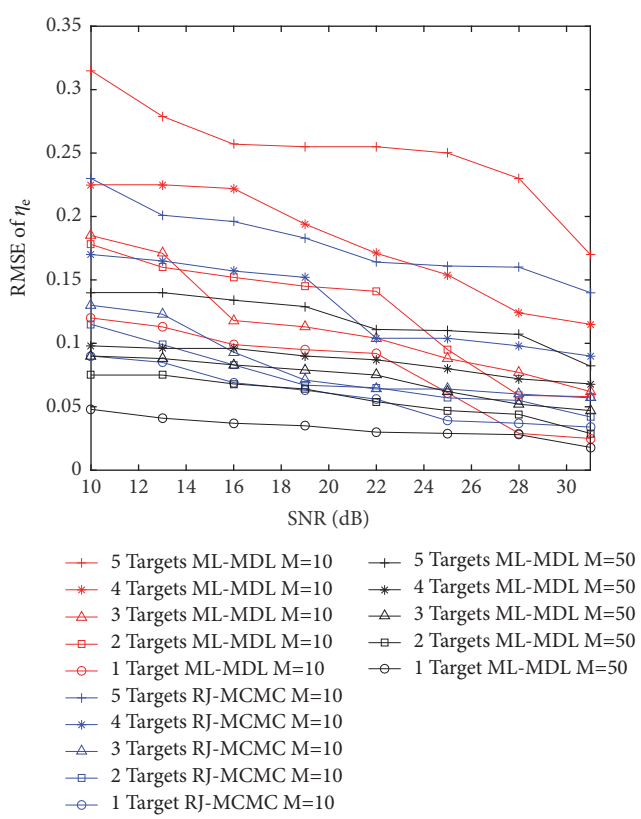

Figure 6: RMSE of η_e estimation under the same power, different target numbers, and different SNR conditions.

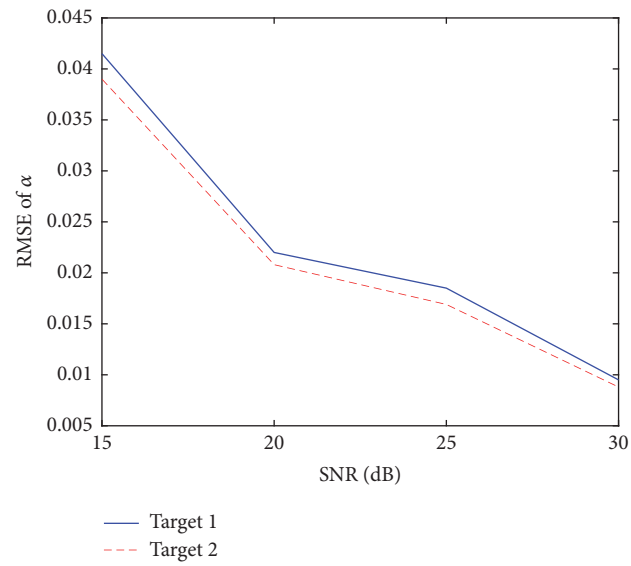

Figure 7: RMSE of α estimation of target 1 and target 2 under the different power, and different SNR conditions.

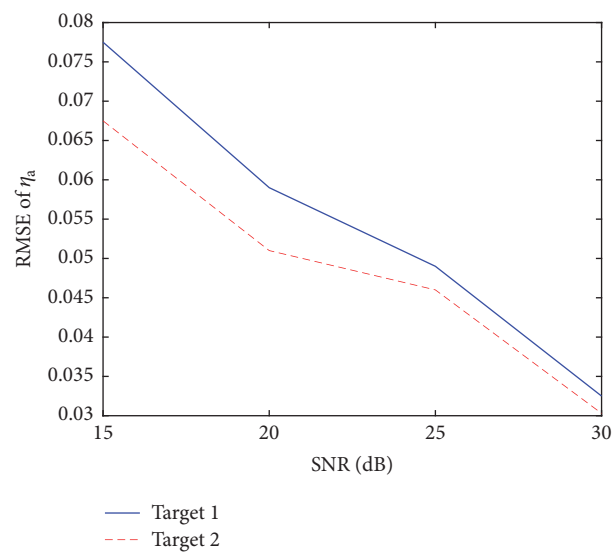

Figure 8: RMSE of η_a estimation of target 1 and target 2 under the different power, and different SNR conditions.

and SNR of target 2 varies from 17dB to 32dB. Every 5dB results are achieved across 200 Monte-Carlo simulation, as shown in Figures 7–9. In the diagram, the SNR of the abscissa represents the SNR of target 1.

As can be seen from Figures 7–9, when there are two targets with different power and when the target SNR is greater than 15dB, the target's relative distance, azimuth, and pitch angle of the target in the subwave gate can be, respectively, 0.045, 0.08, and 0.09, respectively. And obviously, the parameter estimation accuracy of the target with larger SNR is better than that of the target with smaller SNR.

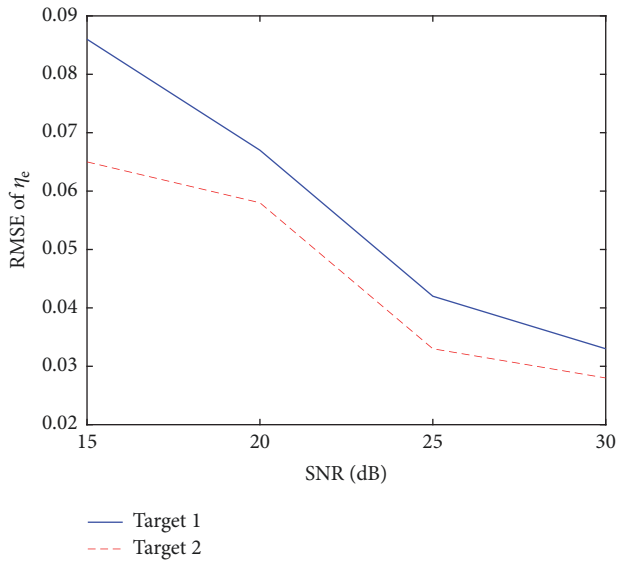

Figure 9: RMSE of η_e estimation of target 1 and target 2 under the different power, and different SNR conditions.

Both the proposed algorithm and the ML-MDL algorithm are the concrete implementation of MCMC algorithm. The computational complexity of the two methods corresponds, mainly depending on the number of subpulses M. However, as can be seen from Figures 7–9, the estimation performance of RJ-MCMC method under 10 subpulses is between the other two cases. That is to say, compared with ML-MDL method, RJ-MCMC method has better estimation performance under the same number of subpulses. This also means that compared with ML-MDL method, RJ-MCMC method needs less observation time to obtain the same or similar estimation accuracy as ML-MDL method, which is of great significance for real-time processing.

6. Conclusions

In this paper, we propose a multiple parameter estimation method based on RJ-MCMC for multiple nondiscernible targets. Different from the traditional estimation methods, we need to estimate the target parameters and then estimate the order of the model (the number of the targets). The proposed method can simultaneously complete the joint estimation of the target number and the target location parameters. More importantly, the method proposed in this chapter is applicable to many situations with different power and nondistinguishable target. The simulation results show that the method proposed in this chapter requires less observation time to obtain similar and even better estimation performance than the ML-MDL method, which is of great significance for real-time processing.

Data Availability

The data in this paper are mainly some actual measurement interference data. The interference data used to support the findings of this study are available from the corresponding author upon request. Data are research results with intellectual property, so there are some restrictions on data access.

Conflicts of Interest

No potential conflicts of interest were reported by the authors.

Authors' Contributions

Jian Gong and Hui Yuan designed the algorithm scheme. Jian Gong performed the experiments and analysed the experiment results. Qun Wan, Hui Yuan, and Yiduo Guo contributed to the manuscript drafting and critical revision. All authors read and approved the final manuscript.

Acknowledgments

This work was supported by the National Natural Science Foundation of China under Grant nos. 61601502 and 61501501.

References

[1] H. Yuan, C.-Y. Wang, X. Li, and L. An, "A Method against Interrupted-Sampling Repeater Jamming Based on Energy Function Detection and Band-Pass Filtering," *International Journal of Antennas and Propagation*, vol. 2017, no. 1, pp. 1–9, 2017.

[2] T. Liu, X. Wei, and L. Li, "Multiple-element retrodirective cross-eye jamming against amplitude-comparison monopulse radar," in *Proceedings of the 2014 12th IEEE International Conference on Signal Processing, ICSP 2014*, pp. 2135–2140, China, October 2014.

[3] S.-Y. Liu, C.-X. Dong, J. Xu, G.-Q. Zhao, and Y.-T. Zhu, "Analysis of Rotating Cross-Eye Jamming," *IEEE Antennas and Wireless Propagation Letters*, vol. 14, pp. 939–942, 2015.

[4] G. Lu and B. Tang, "Deception jammer rejection using pulse diversity in joint slow/fast-time domain," *Journal of the Chinese Institute of Engineers*, vol. 39, no. 6, pp. 722–726, 2016.

[5] E. Zheng, X. Chen, H. Yu, and C. Sun, "Robust high-resolution beam-forming based on high order cross sensor processing method," *Journal of Systems Engineering and Electronics*, vol. 26, no. 5, pp. 932–940, 2015.

[6] W. R. Gilks and G. O. Roberts, "Strategies for improving MCMC," in *Markov Chain Monte Carlo in Practice [M]*, pp. 49–54, Chapman & Hall, London, UK, 1996.

[7] S. Sherman M and K. Barton D, *Monopulse Principles And Techniques [M]*, Artech House, MA, USA, 2011.

[8] W. D. Blair and M. Brandt-Pearce, "Monopulse DOA estimation of two unresolved Rayleigh targets," *IEEE Transactions on Aerospace and Electronic Systems*, vol. 37, no. 2, pp. 452–469, 2001.

[9] S. Xu, J. Ma, L. Wu et al., "Angular resolving of two closely spaced jammers based on average AOA [C]," in *International Conference on Intelligent Science and Intelligent Data Engineering*, pp. 693–698, Springer Berlin Heidelberg, 2011.

[10] G. C. Brown, W. D. Blair, T. L. Ogle et al., "Statistical AOA estimates with merged measurements from monopulse data

[C]," in *Proceedings of the SPIE Conference on Signal and Data Processing of Small Targets*, vol. 1, pp. 41–45, 2003.

[11] X. Zhang, P. K. Willett, and Y. Bar-Shalom, "Monopulse radar detection and localization of multiple unresolved targets via joint bin processing," *IEEE Transactions on Signal Processing*, vol. 53, no. 4, pp. 1225–1236, 2005.

[12] Z. Lu, M. Gao, H. Jiang, and J. Yan, "Closed-form solutions for directions of two steady targets with two pulses in monopulse radar," in *Proceedings of the 2012 IEEE Radar Conference: Ubiquitous Radar, RADARCON 2012*, pp. 0074–0078, USA, May 2012.

[13] K. J. Parker and M. A. Alonso, "Longitudinal iso-phase condition and needle pulses," *Optics Express*, vol. 24, no. 25, pp. 28669–28677, 2016.

[14] X. Zhang, P. K. Willett, and Y. Bar-Shalom, "Detection and localization of multiple unresolved targets via joint multiple-bin processing [C]," in *Proceedings of the 2003 IEEE Radar Conference*, pp. 232–237, 2003.

[15] J.-R. Larocque and J. P. Reilly, "Reversible jump MCMC for joint detection and estimation of sources in colored noise," *IEEE Transactions on Signal Processing*, vol. 50, no. 2, pp. 231–240, 2002.

[16] A. Isaac, P. Willett, and Y. Bar-Shalom, "MCMC methods for tracking two closely spaced targets using monopulse radar channel signals," *IET Radar, Sonar & Navigation*, vol. 1, no. 3, pp. 221–229, 2007.

[17] Q. Cai, *Research on Separation of Signal Components of Multicomponent Signal [D]*, University of Electronic Science and Technology of China, Chengdu, China, 2005.